Internet of Things 19 (2022) 100541

Contents lists available at ScienceDirect

Internet of Things

journal homepage: www.elsevier.com/locate/iot

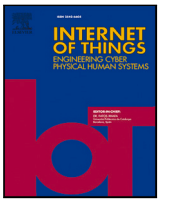

Research article

In-home Health Monitoring using Floor-based Gait Tracking

Katie S. Hahm, Brian W. Anthony *

Massachusetts Institute of Technology, 77 Massachusetts Ave, Cambridge, MA 02139, United States

ARTICLE INFO

Keywords:
Gait monitoring
Smart home
Signal processing
Localization
Ground reaction force

ABSTRACT

Gait assessments are commonly used for clinical evaluations of neurocognitive disease progression and general wellness. However, gait measurements in clinical settings do not accurately reflect gait in daily life. We present a non-wearable and unobtrusive method of detecting gait parameters in the home through the vibrations in the floor created by footfalls. Gait characteristics and gait asymmetry are estimated despite a low sensor density of 6.7 m^2/sensor. Features from each footfall vibration signal is extracted and used to estimate gait parameters with gradient boosting regression and probabilistic models. Temporal gait asymmetry, locations of the footfalls, and peak tibial acceleration asymmetry can be predicted with a root mean square error of 0.013 s, 0.42 m, and 0.34 g respectively. This system allows for continuous at-home monitoring of gait which aids in early detection of gait anomalies.

1. Introduction

Gait characteristics and their change over time have been shown to correlate with an individual's general health. Gait tracking can enable early detection of neurodegenerative diseases [1]. In early stages of Parkinson's disease, patients showed symptoms of asymmetrical gait despite reporting no pain [2]. In cognitively normal adults, higher gait variability correlated with a 12-fold higher risk of mild cognitive impairment, and changes in spatio-temporal gait characteristics correlated with the severity of frailty [3,4]. In addition to its potential for early detection of neurodegenerative diseases, gait characteristics can be informative of an individual's mental health. Depression has been associated with alterations in locomotion [5]. Gait speed has been shown to predict depressive symptoms [6]. Therefore, quantifying gait characteristics and continuous monitoring of gait over time can be valuable for early detection and effective intervention.

While monitoring gait has been shown to be clinically useful, the setting in which gait is evaluated can alter gait measurements. A study tracked the gait patterns of patients with cerebral palsy (CP) and of healthy controls (TD) both inside and outside of the laboratory setting. The results demonstrated that, for both CP and TD groups, most gait characteristics measured in the laboratory significantly differed from those measured outside the laboratory [7]. The CP patients' gait performed better in clinical setting measurements [7]. As a result of the disparity between clinical gait measurement and gait during a daily life setting, there is a significant need for an ambulatory monitoring system to track natural daily activities outside of the clinical setting.

Proliferation of Internet-of-Things (IoT) sensor networks has provided opportunity for new development in applications such as disaster management [8], healthcare [9], and smart cities [10]. Miniaturization and networking of IoT sensors have led to significant interest in their use for human movement tracking, and have raised interest in new smart home capabilities [11]. Within the growing field of ambient intelligence, which explores the interaction between sensed environments and their inhabitants, smart sensor technologies deployed in a home can be used to monitor the resident's well-being [12]. Many advancements in IoT maintain a low barrier to deployment and is minimally intrusive. For example, IoT technologies have been used to increase the independence

* Corresponding author.
E-mail addresses: khahm@mit.edu (K.S. Hahm), banthony@mit.edu (B.W. Anthony).

https://doi.org/10.1016/j.iot.2022.100541
Received 11 February 2022; Received in revised form 2 May 2022; Accepted 4 May 2022
Available online 16 May 2022

of the elderly and disabled people through autonomous smart home approaches and increased security through non-wearable sensor systems [13,14].

1.1. Floor sensing approach

Our system uses four single-axis accelerometers placed on the floor to acquire transient footstep vibrations. The theory behind this approach is that vibrations traveling through a medium can deliver information about the characteristics of a footfall impact. Relevant features from the impact are extracted from the accelerometer signal. Machine learning algorithms and probabilistic models use these features for gait analysis and interpretation. This continuously powered, ambient system is a minimally invasive approach to monitoring the gait of the resident. We present algorithms to extract clinically important gait parameters from footfall induced vibrations, and we quantify performance accuracy by comparing the estimates to standard measurements obtained from camera-based motion capture, inertial measurement units, and force sensitive resistors.

In this paper, we demonstrate an approach for monitoring a subject's gait characteristics by using the natural interactions between the resident and the home — the floor vibrations from footfalls. In Section 2, the gait parameters of interest are discussed. In Section 3, signal feature extraction of a given footfall vibration signal is shown. In Section 4, estimating step times of each leg by using the extracted features is discussed. In Section 5, estimating locations of footfalls to ultimately estimate the tibial acceleration of each leg is discussed. In Section 6, the estimation algorithm results of step times, location, and tibial acceleration are shown, and the performance of each estimation is evaluated against the ground truth measurements.

2. Previous work

Researchers have demonstrated that gait quantification is possible outside of the clinical setting using wearable technologies. For example, infrared motion capture with body-worn tags were used to detect falls [15]. Instrumented insoles with pressure sensors and inertial sensors were integrated with shoes for gait analysis [1]. Despite being mobile, this approach relies on the user to insert the sensors in their shoes correctly and recharge them as necessary. Requiring the subject to use and correctly mount these pressure sensors can be challenging, especially for users with physical limitations.

Non-wearable systems have been used to estimate gait characteristics in living environments. Infrared thermography creates visual images of the person and uses image tracking to recognize human gait patterns [16]. Cameras have been used to extract joint movements without placing markers on the subject for gait recognition [17]. However, these visual-based methods raise privacy concerns when continuously implemented in the home. WifiU uses WiFi signals to capture gait patterns and resolves some privacy issues; however, this system is only applicable for identifying gait on predefined paths [18]. Floor-based approaches have also been used for gait detection. Resistive sensor arrays with a sensor density of 1024 sensors/m^2 have been used to design a sensor floor mat to extract gait parameters [19]. A series of 30 cm $\times$ 30 cm tiles with a load sensor at each corner were placed to cover the floor to localize the home residents [12]. These floor sensor arrays, although successful in extracting gait characteristics, must replace pre-existing flooring in homes and require a high sensor density, which can make deployment and scalability more challenging.

2.1. Gait parameters of interest

A range of gait parameters are indicators of health [1]. We demonstrate a floor accelerometer system to estimate the following clinically important parameters:

1. Step time: The time between the heel strike of one foot to the heel strike of the contralateral foot. Left-to-right step time and right-to-left step time can be different, resulting in asymmetric step time.
2. Ground reaction force (GRF): The kinetic gait parameter that measures the forces from the ground that produce movement.

Step time variability is useful to predict falls and correlates with factors such as strength, balance, and mental health [20]. Step time asymmetry requires increased metabolic power, has higher mechanical costs, and is correlated with strength asymmetry [21,22]. Significant step time asymmetry and variability is reported in stroke survivors and individuals with chronic stroke [23,24]. GRF has been shown to be a marker for Parkinson's disease and is also used to facilitate performance improvement and enhance injury management [11,25]. Therefore, step time and GRF are important parameters to continuously monitor outside of the clinical setting. Using subject testing and analysis, we demonstrate that the floor accelerometer system can estimate step time, step time asymmetry, and ground reaction forces.

3. Experimental methodology

We collected data using a series of walking sessions with different interventions. Our interventions focused on inducing step time variability and asymmetry as well as variations in ground reaction forces on otherwise healthy individuals. Subjects were encouraged to walk naturally despite these interventions.

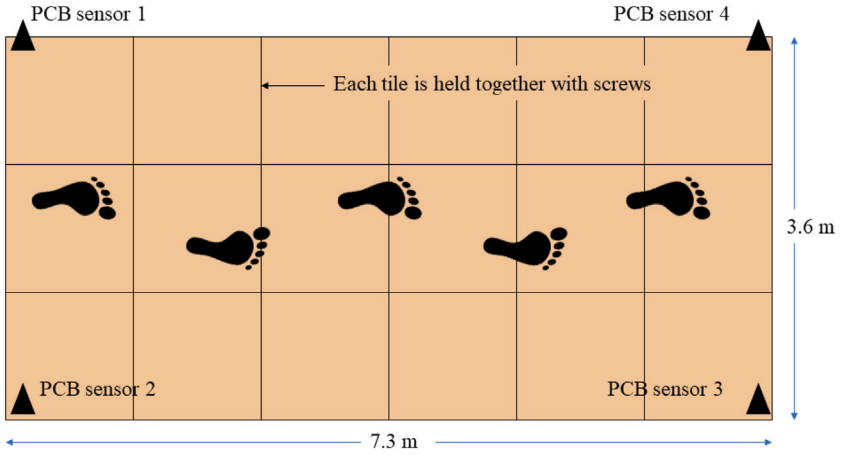

Fig. 1. The floor is made from 18 wood tiles joined together in a 3 × 6 grid to form a 7.3 m × 3.6 m floor. Accelerometer sensors are placed in the corners of the floor and the subjects are instructed to walk across the floor.

Table 1
Descriptions of interventions during experiment. The interventions were given in this order.

Intervention	Description
1	Regular walking (no intervention)
2	Wearing a brace on the right knee
3	Repeat intervention 2
4	Wearing an insole in the right shoe and carrying a comfortable but significant weight on the left hand
5	Repeat intervention 4
6	Regular walking (no intervention)

3.1. Experimental procedure and data collection

This study was performed under Committee on the Use of Humans as Experimental Subjects (COUHES) protocol 2011000269. All volunteers were healthy adults, 3 males and 2 females with weight ranging from 50 kg to 68 kg and height ranging from 1.57 m to 1.8 m. Each subject was given minimalist trail runner shoes by Whitin (Seattle, WA) in their best fitting size. These shoes are minimally supported to avoid cushioning effects.

Each subject was asked to walk for 2 min back and forth on the testing floor. The path was not predetermined, and the only instruction was to walk back and forth along the long-axes of the floor. The subjects were instructed to walk naturally at a speed that was comfortable. The subjects repeated this walk with various interventions. When turning at the end of the floor, the subjects could take a break for a few seconds. Between different interventions, the subjects could take a break for as long as they wished.

The interventions are shown in Table 1. The brace was a 3-panel knee immobilizer by United Ortho (Fort Wayne, IN). The weight was an adjustable dumbbell and was changed to suit the strength and comfort of each subject which ranged between 6.5 kg to 11.5 kg. The insole is a 2.5 cm silicone heel lift insole from Wakafit (Dongguan, China).

3.2. System hardware

Each modular floor square is made of birchwood of size 1.2 m × 1.2 m. The squares were fixtured together similar to a real home floor, as typical homes are constructed with different substructures that make the vibrations in the floor travel through nonuniform mediums. Our floor size is 3.6 m × 7.3 m. The floor dimensions were chosen such that it is similar to a typical room size [26]. An illustration of the experimental floor is shown in Fig. 1.

Four high sensitivity low frequency seismic accelerometers by PCB Piezotronics (Depew, NY) model 393A03 were placed in the corners of the floor. A diagram of the floor is shown in Fig. 1. The data from these sensors was collected through National Instruments (NI) (Austin, Texas) model cDAQ-9174 and NI 9230 data acquisition modules. The sampling frequency was 12.8 kHz. This equates to a sensor density of 6.7 m^2/sensor.

To obtain our ground truth measurements, we used three wearable sensors as reference systems and compared their data to the estimations from the floor vibration approach. The Trigno Research+ system by Delsys (Natick, Massachusetts) was used to obtain timing and tibial acceleration data. The Interlink Electronics Force Sensitive Resistor (FSR) attached to the Trigno system was placed in the heel of each foot to measure the timing of the heel strike. The sampling rate for the FSRs was 296.3 Hz and each FSR was 2.5 cm in diameter. The FSR has actuation force of 0.1N and has a device rise time of <3 microseconds. Although these

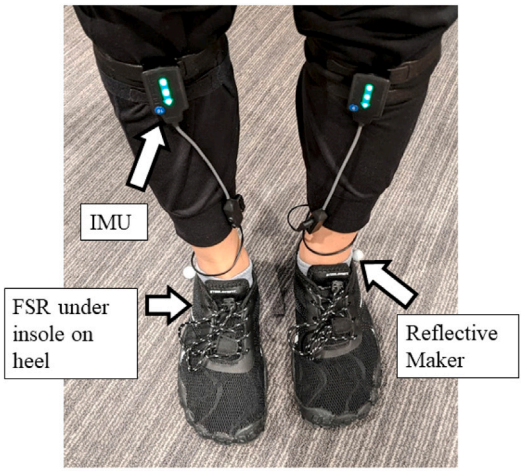

Fig. 2. The IMU, FSR, and reflective marker attached to the subject used to measure the ground truth values to evaluate performance of the floor vibration approach. Elastic straps hold the IMU in place, and tape holds both the FSR and marker in place. The wire was placed to not impede in the subject's walking.

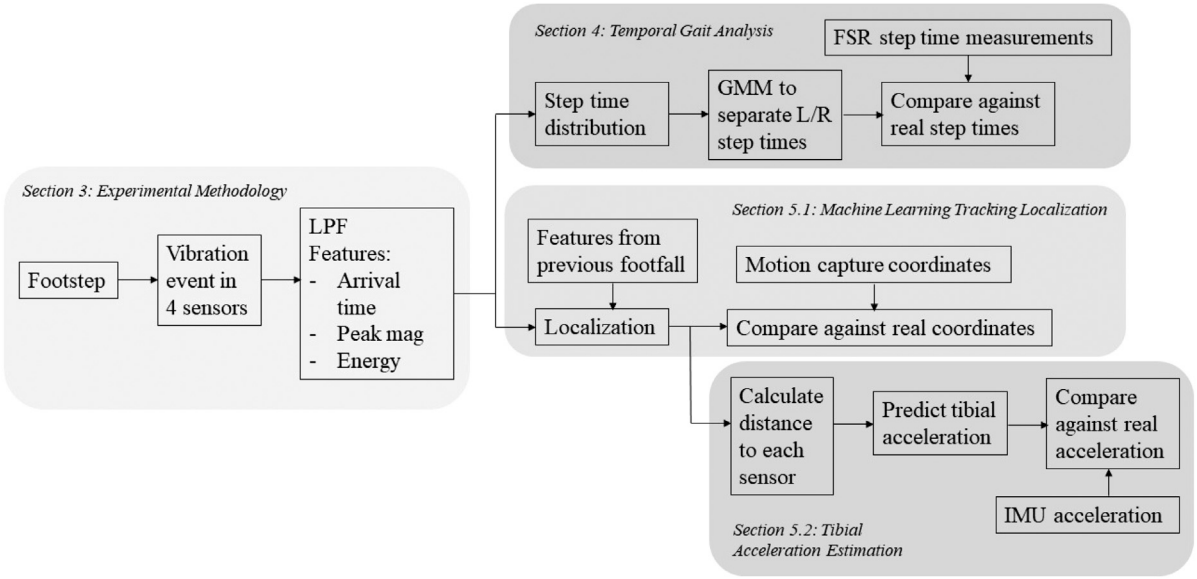

Fig. 3. Block diagram outlining the process of using floor vibrations to extract step time, location, and tibial acceleration of footfalls. When a footstep event is detected, the signal is filtered and processed to extract signal features. These signal features are used to estimate step times, location, and tibial acceleration. We use ground truth measurements from FSRs, motion capture, and IMUs to evaluate the performance of using these extracted features to estimate gait parameters.

device characteristics may affect the ground truth measurements, the error in timing measurement is very small and thus negligible. FSRs placed in insoles have been widely used to measure gait cycle timing [27]. The Trigno module inertial measurement units (IMUs) was placed on the tibia of both legs by securing with elastic Velcro straps to measure the tibial acceleration. The IMUs had sensitivity of ± 8 g, and had sampling frequency 148.1 Hz. The IMU module weighed 19 grams. IMUs are one of the most widely used sensors for gait analysis, and have been used to quantify asymmetry [1]. This placement of IMUs have been used to measure gait force characteristics [28]. The OptiTrack Motive motion capture system (Corvallis, OR) was used by placing a reflective node on the side of the heel to measure the ground truth location measurement of the foot. The motion capture sampling frequency was 180 Hz. The motion capture has marker location accuracy under 1 mm, and thus location measurement error is negligible in using as a reference sensor. These sensor configurations are shown in Fig. 2. The data was recorded in the Immersion Lab in MIT.Nano building 12 at the Massachusetts Institute of Technology.

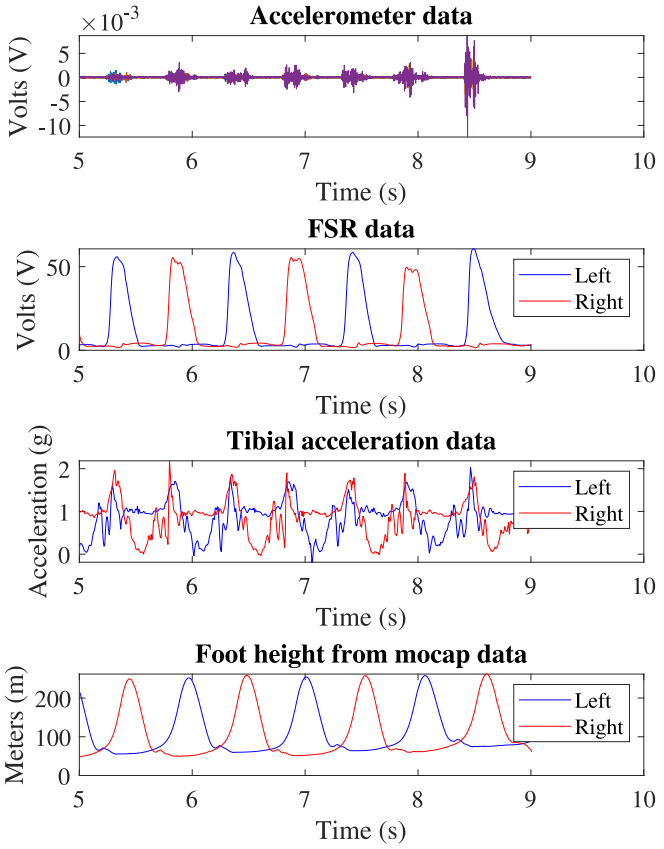

Fig. 4. Raw signals of the accelerometers, FSRs, IMU, and motion capture.

3.3. Gait feature extraction

The gait feature extraction approach and gait analysis process is illustrated in Fig. 3, and outlines the sections of this paper. The peaks of each footfall are found using windowing to locate the footstep vibration events. This accelerometer signal is then filtered with a finite impulse response (FIR) lowpass filter with cutoff frequency of 1920 Hz to remove noise. An example of the raw signals for the accelerometers, FSR sensors, IMUs, and motion capture is shown in Fig. 4.

Each footfall impact resulted in a window of oscillation for each sensor. The Akaike Information Criterion (AIC) picker was used on this window to find the arrival time of each footfall [29]. Spline interpolation over local maxima separated by 300 samples was used to find the upper and lower peak envelopes of this window. End time of the impact was determined by when the envelope meets the noise threshold. From each vibration signal, 12 values were extracted for each footfall - 3 values from each of the 4 sensors. The following parameters are defined for each window corresponding to each impact, and are illustrated in Fig. 5 for further clarity. i notates the sensor number and n notates the footfall number.

1. Arrival time differences: The sensor closest to the footfall usually detects the vibration first. This value is used as a reference to calculate the arrival time differences between the other three sensors. The four arrival time difference values for each impact were obtained as follows:

$$\Delta t_i^n = t_i(k_{0,i}^n) - \min[t_1(k_{0,1}^n), t_2(k_{0,2}^n)...t_4(k_{0,4}^n)] \tag{1}$$

   where Δt_i^n is the arrival time difference at sensor i and footfall window n, and $t_i(k_{0,i}^n)$ is the arrival time of sensor i at footfall window number n and sample number $k_{0,i}^n$. Note that the sensor that detects the vibration first has an arrival time difference of 0.
2. Peak magnitudes: For each of the 4 sensors, the peak voltage value of the absolute value of the impact signal window was recorded.
3. Energy: For each of the 4 sensors, the energy of the signal was obtained as follows:

$$e_i^n = \sum_{k=k_{0,i}^n}^{k_{0,i}^n + K_i^n} z_i(k)^2 \tag{2}$$

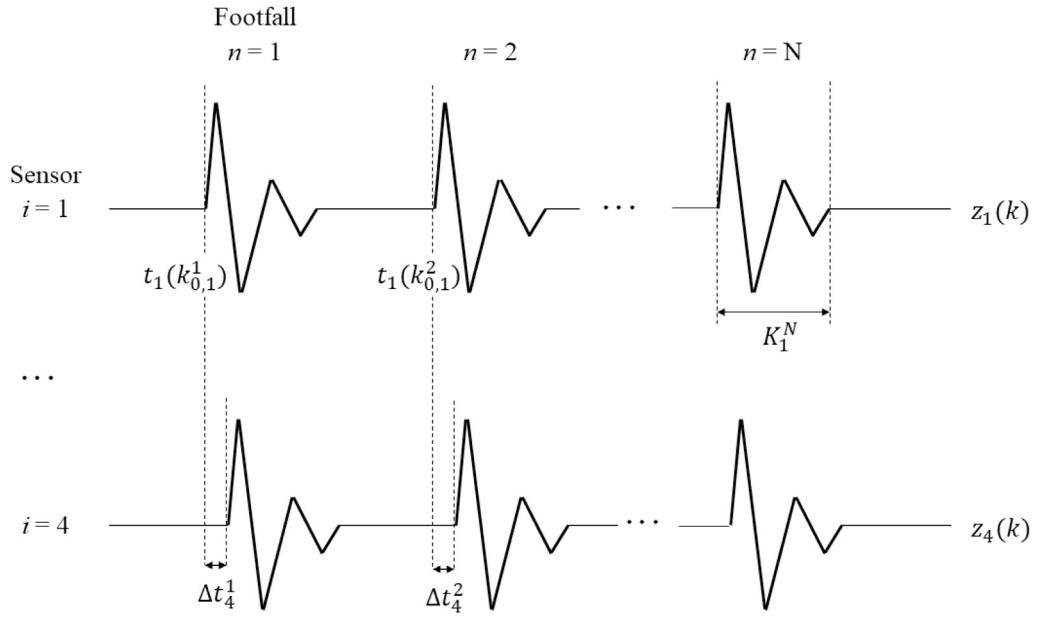

Fig. 5. An illustration of the variables corresponding to the signal for clarity.

where K_i^n is the number of samples in the signal window.

The FSR sensors were used to obtain the ground truth heel strike times of the left and right foot. A find-peaks algorithm was used to extract each heel strike, and the same AIC-picker algorithm was used to extract the start time of each heel strike.

The maximum tibial acceleration was detected by the IMUs within a window at the heel strike time. We obtained the coordinates of the foot at the footfall time by using motion capture.

4. Temporal gait analysis

The average step time can be directly computed from the floor accelerometers using the following equation:

$$\text{Average step time} = \left(\sum_{n=2}^{N} \min[t_1(k^n_{0,1})...t_4(k^n_{0,4})] - \min[t_1(k^{n-1}_{0,1})...t_4(k^{n-1}_{0,4})] \right) / (N-1) \tag{3}$$

The cadence of the subject is directly computed by counting the average number of steps in one minute. When compared to the ground truth measurement from the FSR sensors, the floor accelerometers have an average step time estimation error of 0.1 ms and a cadence estimation error of 0.0135 steps/min.

Estimating step time variability and asymmetry is more challenging. The biggest constraint lies in being unable to distinguish between the left and right foot. A resident may use a different foot to start the walking episode each time, so we cannot identify each impact as the left or right foot. Moreover, in a home a resident typically starts and stops walking frequently and does not take many steps in each walking episode. This may be due to the furniture or the size of the rooms. This prevents using a single walking episode (without turns or stops) to determine if there is any step time asymmetry, as step times are also variable. There is a need to combine the different walking episodes to evaluate average step time asymmetry over time without distinguishing between the left and right leg.

Previously, the need to label left and right footfalls was bypassed by looking at the distributions of all step times [30]. Walks with a limp were demonstrated to have a larger standard deviation and higher bimodality coefficient when compared to symmetric walks. This analysis is extended to extract the values of left and right step times to further quantify the limp.

4.1. Asymmetric step time extraction

To extract the left and right step times, we use a Gaussian mixture model (GMM) on the step time distribution to split the data into two Gaussian distributions [31]. An example is shown in Fig. 6. This relies on the assumption that the dataset approximately has the same number of left and right footsteps, which results in the GMM mixture weights being equal. However, when the walk is symmetric and there is no limp, the GMM is unable to split the dataset into two subsets because the left and right step times are less distinguishable. This results in unequal mixture weights. Let μ_1 be the mean of GMM component 1, ϕ_1 be the mixture weight

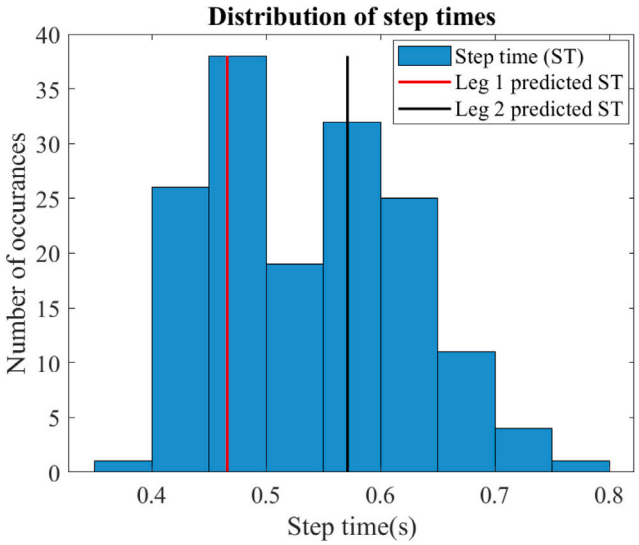

Fig. 6. Step time distributions of one subject during a limping walk with a knee brace. The GMM model predictions are shown to extract the two different average step times.

of GMM component 1, s_f be the calculated scaling factor, and μ_1' be the scaled mean of component 1. We implement a scaling algorithm as follows:

$$\mu_1' = \mu_1 + (\mu_2 - \mu_1) \times s_f \tag{4}$$

$$\text{Let } \phi_{max} = \max[\phi_1, \phi_2], \qquad s_f = \begin{cases} 1 - \phi_1^2, & \text{if } \phi_{max} > 0.75 \\ |0.5 - \phi_1|, & \text{otherwise} \end{cases} \tag{5}$$

μ_2' can be calculated using the same equations as above. Using this algorithm, a final scaled mean for the two subsets is defined to predict the left and right step times.

5. Ground reaction force analysis

In detecting ground reaction forces (GRF) during footfalls, the gold standard has been to use force plates [28]. Because a force plate must be mounted on the floor, it is not possible for us to verify the floor's performance using a force plate, as the footstep will not fall on the wooden floor. However, there are ample research that have demonstrated the efficacy of using wearable IMUs to estimate the GRF. One such method uses the peak tibial acceleration (TA) of the shank of the leg to estimate the peak GRF [28]. These methods have adequately predicted the GRF and achieved a mean absolute error of 5.2% of body weight [32]. To estimate GRF using our floor, we will use the TA as the prediction goal.

5.1. Machine learning tracking localization

To find the TA using the vibration signals from the floor, the peak magnitudes and energy of each footfall are correlated to the peak TA. However, the floor dampens the vibrations and thus the magnitudes and energy of each impact is weakened the farther away an impact is located, as illustrated in Fig. 7. Therefore, the location of the footfall is first estimated and used to appropriately scale the extracted signal features to ultimately predict TA.

Our approach extends the previous localization methods by incorporating a tracking approach in our algorithm to estimate the exact coordinates of the footfall. We use the precondition that each subsequent step will be in proximity to the previous step. Our training set incorporates this tracking method and has features as shown in Table 2.

Features 1–5 from Table 2 has 4 values from the 4 different sensors, and feature 6 has one value, so there are 21 features in total. The first step of each walking segment does not have a previous step, so only features 1–3 from Table 2 are used to predict the first steps. Each footstep is predicted one at a time, and the previous prediction is used as feature 21 — the previous coordinate. The ratio of the previous footfall's peak magnitude and energy to the current footfall's peak magnitude and energy of each sensor is used as features to further inform the direction of the step taken. In this way, the localization approach not only uses features from the vibration signal, but also uses a tracking approach. Gradient boosting regression (GBR) was used with 10-fold cross validation to maximize the size of the dataset. Randomized search with 25 iterations was used for hyperparameter optimization. Ground truth coordinate values were extracted from the motion capture data to measure the performance of our tracking localization approach.

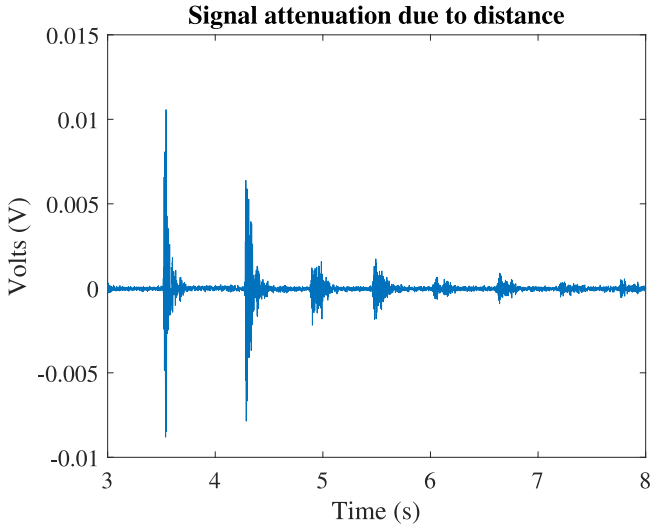

Fig. 7. Example of signal attenuating due to the distance between the footfall and sensor placement. The subject walked away from the sensor.

Table 2
Features extracted from footfall vibration signal for estimating location.

Feature	Description
1	Arrival time differences
2	Peak magnitudes
3	Energy
4	Ratio of current peak magnitudes to previous peak magnitudes
5	Ratio of current energy to previous energy
6	Estimated previous coordinate

Table 3
Features extracted from footfall vibration signal for estimating TA.

Feature	Description
1	Distance of the impact to each sensor from estimated location
2	Peak magnitudes
3	Energy

5.2. Tibial acceleration estimation

Given the predicted locations as demonstrated above, the distance of the impact to each sensor is calculated as the sensor locations are known and fixed. The features shown in Table 3 are used to estimate peak TA.

This approach uses 12 total features – 3 features from each of the 4 sensors – to estimate the TA. Although the dataset from the interventions were combined, the dataset from each subject were kept separate to avoid differences in signal due to weight or walking style. The left and right foot are assumed to have the same mass, and thus would produce the same vibration signal from the same TA and same location. The interventions showed a range of TA as shown by Fig. 8. Given the range of average TA of each foot across different interventions, we can evaluate the performance of the TA estimation algorithm in analyzing both symmetric and more asymmetric walks.

GBR is used to estimate the TA with 5-fold cross validation and randomized search is used with 25 iterations for parameter optimization. These predictions were compared against the ground truth data measured from the IMUs placed on the tibia. Given these predictions, we used K-Means clustering with 2 clusters to separate the estimated values to find the estimated average TA for each leg.

6. Results and discussion

In this section, the results from the step time asymmetry, localization, and TA prediction approaches are presented and compared to the ground truth measurements.

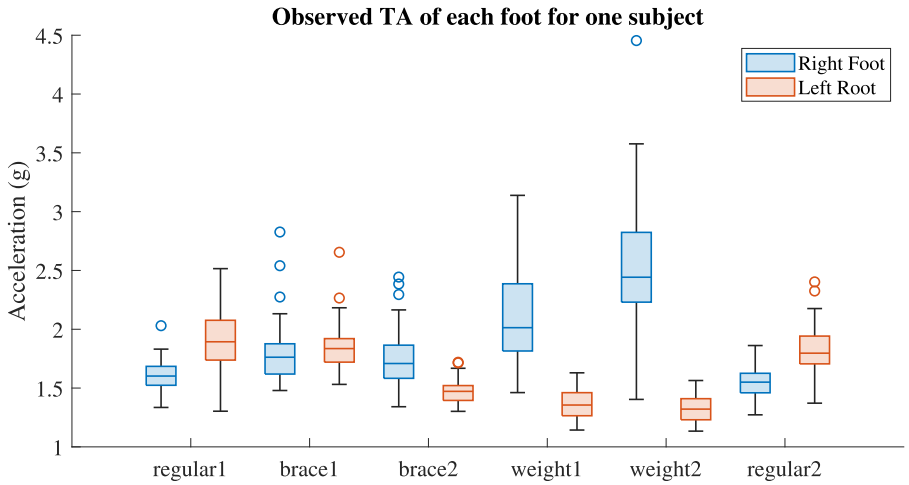

Fig. 8. Box charts of observed average TA of left and right leg between different interventions for one subject obtained from ground truth IMU reference sensors. The TA was similar between the left and right leg on all interventions except when using the weight and insole, in which the left leg had higher TA compared to the right leg. With this variation in TA, we are able to evaluate our TA estimation approach for both symmetric and asymmetric TA.

Table 4
Measured left and right step time compared against the results from the GMM for all interventions as listed in Table 1. The scaled means are similar to the measured means, which can predict the presence of an asymmetry and estimate the step times of each leg.

Intervention	Real m1	Real m2	GMM m1	GMM m2	GMM p1	GMM p2	Scaled m1	Scaled m2
1	0.53 s	0.54 s	0.53 s	0.59 s	0.94	0.06	0.53 s	0.53 s
2	0.71 s	0.60 s	0.72 s	0.59 s	0.56	0.44	0.71 s	0.59 s
3	0.57 s	0.72 s	0.57 s	0.72 s	0.47	0.53	0.57 s	0.71 s
4	0.51 s	0.52 s	0.51 s	0.51 s	0.77	0.23	0.51 s	0.51 s
5	0.47 s	0.49 s	0.52 s	0.48 s	0.14	0.86	0.48 s	0.49 s
6	0.49 s	0.51 s	0.50 s	0.60 s	0.98	0.02	0.50 s	0.49 s

6.1. Asymmetric step time estimation

The results of the GMM evaluation of step times for one example subject with all interventions are shown in Table 4. Table 4 shows that the subject had very similar mean step times between their left and right legs during their regular walking and when walking with the insole and weight. Their step time was asymmetric for the braced knee interventions. Some GMM mixture weights are not even and thus the GMM mixture means are not accurate. After using the scaling algorithm, the scaled predicted means are similar to the measured step time means for all interventions. With this approach, an average left and right step time estimation root mean square error (RMSE) of 0.0125 s across all interventions and all subjects is achieved. The results from all subjects for regular and brace interventions are summarized in Fig. 9. The predicted and measured symmetry indices are similar across all subjects.

6.2. Tracking localization

The tracking localization algorithm performed successfully with an RMSE of 0.42 m across all interventions and all subjects. To compare the tracking localization approach to a baseline approach, the GBR algorithm was run on the same dataset without information about the previous footfall. This baseline approach only used features 1–3 from Table 2. This achieved an average RMSE of 0.83 m across all interventions and all subjects. The tracking localization approach improved the localization algorithm by 49% from the baseline approach. The performance of the tracking localization algorithm on one subject in shown in Fig. 10. The results of this localization algorithm can be used to calculate the predicted distance of each impact to the sensor to estimate TA.

6.3. Tibial acceleration

The TA estimation algorithm using the predicted locations achieved an RMSE of 0.63 g or 24.8% of the average TA. Fig. 11 shows the predicted TA values against the measured TA values in one subject for regular and weight interventions. The K-Means cluster centroids corresponding to the datapoints in Fig. 11 are shown in Table 5.

In the regular walk, the TA values are clustered together, while the weight and insole intervention induced a wider spread of TA values. The centroids in the regular walking are closer together, whereas the centroids in the weight intervention walk are farther apart. Across all subjects, the K-Means clustering centroids for the predicted TA had an average absolute error of 0.34 g, or 13.3%, when compared to the average measured TA.

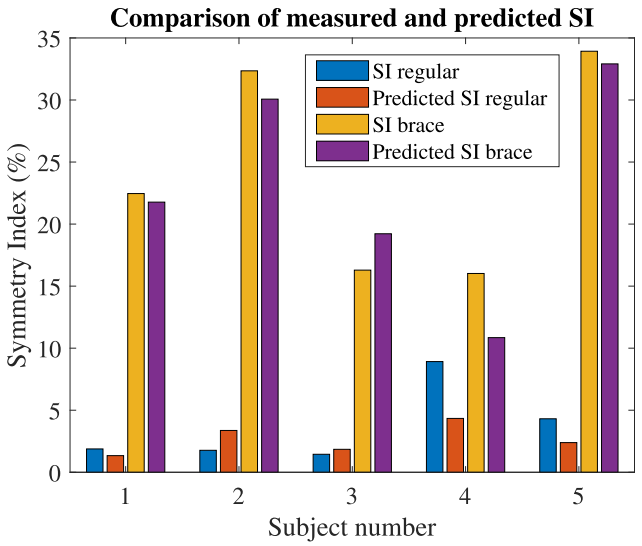

Fig. 9. Comparison of the measured and predicted symmetry index across all subjects for regular walking and knee brace intervention. The regular walking has a much lower SI than the brace walking, and the predicted SI is also able to distinguish between the two walks.

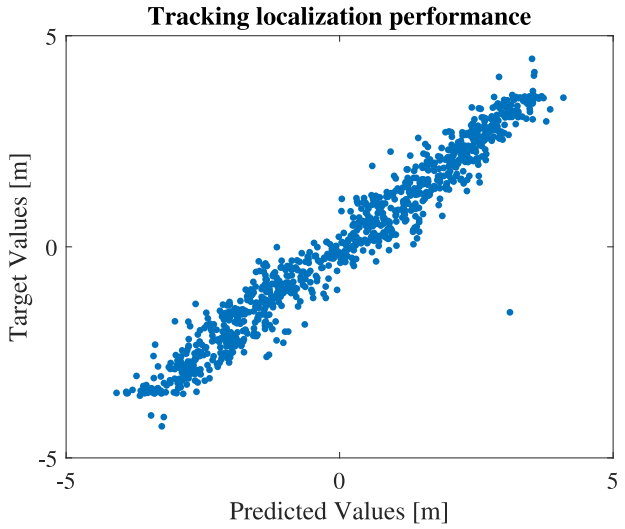

Fig. 10. The predicted location compared against the target location values. The tracking localization algorithm achieves an RMSE of 0.42 m.

Table 5
K-Means centroids of predicted TA compared against the measured TA averages for each leg for one subject. Only the regular and weight & insole interventions are shown as the other interventions had similar left and right TA, as shown by Fig. 8.

Intervention	Predicted TA 1	Predicted TA 2	Measured TA 1	Measured TA 2
Regular	1.62 g	1.95 g	1.61 g	1.91 g
Weight & insole	1.59 g	2.14 g	1.37 g	2.12 g

6.4. Discussion

We demonstrated detection of step time asymmetry with an RMSE of 0.013 s using the Gaussian mixture model on the step time distributions. We do not determine if it is the left or right leg that has the smaller or larger step time. Nevertheless, knowing the presence of a step time asymmetry is important information.

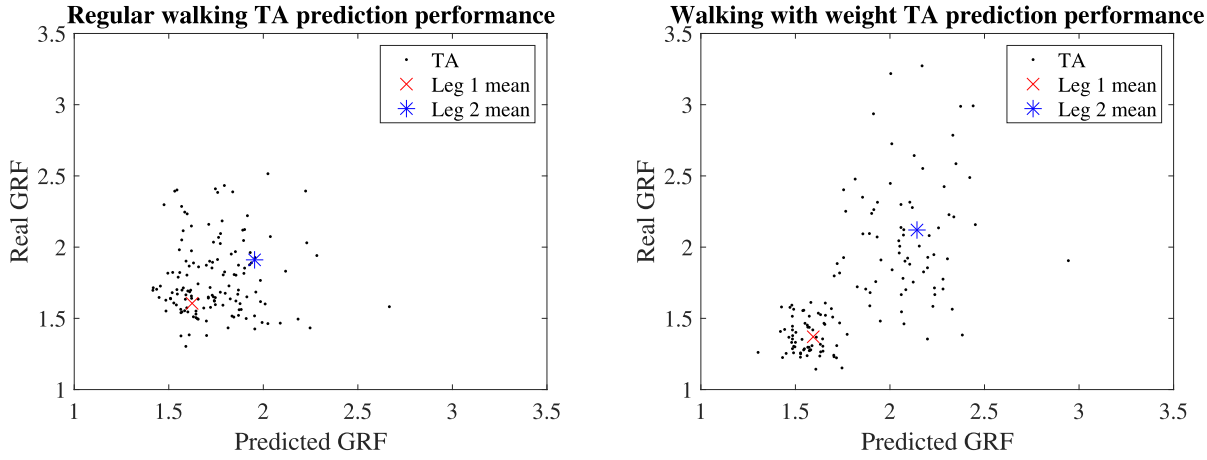

Fig. 11. The predicted TA values compared against the measured target TA values. (a) The regular walk has clustered TA. (b) The walk with the weight and insole has a wider spread of TA values. This indicates that the walk had more asymmetric TA when compared to the regular walk.

We also demonstrated the localization of footfalls with an RMSE of 0.42 m by using a tracking localization method. Previous works localized footfalls with 0.41 m average error [33] and 0.6 m average error [34]. These previous efforts did not use a tracking approach and used a predetermined footfall location for the ground truth location values. By forcing the landing of each step to fall at a specific location, the walking pattern used to test the localization algorithm may be unnatural. Using predetermined paths make the localization problem a classification problem, as there are a finite number of footfall locations to predict. In our work, we do not use predetermined footfall locations and instead use motion capture to determine the ground truth location measurements, thus allowing for a more natural walking data. Our approach uses regression, as the footfall location is only restricted to the size of the floor and is otherwise not predetermined. In this work, we use larger floor spaces with a lower sensor density than previous efforts.

Using the predicted locations to compute the distance of the impact to each sensor, we achieved TA prediction with an RMSE of 0.63 g. We split the predicted group of TA into two clusters. The cluster centroids achieved an RMSE of 0.34 g when compared against average measured TA values of each leg. Having an accurate average TA prediction of each foot is important in tracking any drifts of these values over time.

Both the height and weight of the subject did not correlate with localization and TA estimation performance. The sensors and floor materials showed sufficient sensitivity to extract informative features such as vibration energy across the range of subjects' weights such that weight was not an issue. All subjects were adults, and the floor vibration performance was not tested on much younger individuals who may be lighter.

The author had the opportunity to shadow a neurology doctor at the Beth Israel Deaconess Medical Center during her clinical hours [35]. Dr. VanderHorst corroborates that patients with Parkinson's disease have different gait when in a clinical setting compared to their home environment. Dr. VanderHorst attributes this to multiple factors including an unfamiliar environment, discomfort and fatigue from travel, and awareness of their gait being observed. The recall of the patient's at-home gait characteristics is qualitative; some caretakers remark during a patient's clinical gait assessment that the patient's walking looks different. With our approach to detect average step time, cadence, step time asymmetry, and tibial acceleration asymmetry, we can monitor the resident's gait continuously and detect any changes over time, bridging the disparity between gait evaluated in the clinic and at-home gait.

7. Conclusions

Footfall vibration timing and characterization was used to detect changes in gait parameters over time. As an ambient non-contact system, this approach may reduce limitations associated with subject compliance when compared to wearable systems. This floor sensing system allows for continuous monitoring of clinically important gait parameters, which reveal important aspects of health that were typically difficult to access. Monitoring gait as a biomarker can change how early detection and early intervention care is practiced for neurocognitive diseases with gait related symptoms. It provides a more accurate monitoring of gait in the daily life, which can be different from infrequent clinical gait evaluations. With a low sensor density of 6.7 m^2/sensor, this method is feasible to deploy in homes with minimal privacy issues compared to image-based methods. Step time asymmetry, footfall localization, and peak tibial acceleration asymmetry were estimated from floor vibration signals with root mean square errors of 0.013 s, 0.42 m, and 0.34 g respectively.

7.1. Limitations

Our experiments and results focused on wooden floors, and was not tested on other floor types such as tiles and carpet. However, our algorithms did not incorporate any properties of a wooden floor. Unique signatures of vibration propagation associated with a particular floor are encompassed in the machine learning algorithm. We believe our approach can be extended to other types of flooring. Additional or more sensitive accelerometers may be required.

7.2. Future work

The proposed technique can be improved and extended to perform under conditions of multiple people walking at the same time. Additional features can be extracted from the signal to find more relevant features of the signal, and feature selection techniques can be used to select the most optimal features [36]. The home is often occupied by multiple people. Parsing the received signals and gait parameters of multiple occupants is important for implementation. We demonstrated a localization algorithm useful for GRF estimation. Localizing the resident can have further important applications in the monitoring of daily activities and habits. In-home gait tracking can also be used to track effectiveness of treatments. The dosage of levadopa, a commonly used treatment for Parkinson's disease, is adjusted to suit each patient to reduce stride time variability and gait and dexterity impairment [37,38]. Tracking gait characteristics using floor accelerometers could aid in accurate at-home assessment of the effectiveness of medications.

Declaration of competing interest

The authors declare that they have no known competing financial interests or personal relationships that could have appeared to influence the work reported in this paper.

Acknowledgments

This work was funded by the Sekisui House at MIT program in collaboration with the Institute for Medical Engineering and Science (IMES), the Center for Clinical and Translational Research at MIT, United States, and the Immersion Lab at MIT.Nano, United States. We would like to thank Dr. Veronique VanderHorst MD PhD for her clinical insight and giving us the opportunity to observe Parkinson's disease patients during clinic visits.

References

[1] A. Muro-de-la Herran, B. Garcia-Zapirain, A. Mendez-Zorrilla, Gait analysis methods: an overview of wearable and non-wearable systems, highlighting clinical applications, Sensors 14 (2014) 3362–3394.
[2] A. Mirelman, P. Bonato, R. Camicioli, T.D. Ellis, N. Giladi, J.L. Hamilton, C.J. Hass, J.M. Hausdorff, E. Pelosin, Q.J. Almeida, Gait impairments in Parkinson's disease, Lancet Neurol. 18 (7) (2019) 697–708.
[3] M. Montero-Odasso, S.W. Muir, M. Hall, M. Speechley, Gait variability is associated with frailty in community dwelling older adults, J. Gerontol. A 66 (2011) 568–576.
[4] M. Ritt, S. Schülein, H. Lubrich, L. Bollheimer, C. Sieber, K.-G. Gassmann, High-technology based gait assessment in frail people: associations between spatio-temporal and three-dimensional gait characteristics with frailty status across four different frailty measures, J. Nutr. Health Aging 21 (3) (2017) 346–353.
[5] J. Sanders, M. Bremmer, D. Deeg, A. Beekman, Do depressive symptoms and gait speed impairment predict each other's incidence? A 16-year prospective study in the community, J. Am. Geriatr. Soc. 60 (2012) 1673–1680.
[6] D. Paleacu, A. Shutzman, N. Giladi, T. Herman, E. Simon, J. Hausdorff, Effects of pharmacological therapy on gait and cognitive function in depressed patients, Clin. Neuropharmacol. 30 (2007) 63–71.
[7] L. Carcreff, C.N. Gerber, A. Paraschiv-Ionescu, G. De Coulon, C.J. Newman, K. Aminian, S. Armand, Comparison of gait characteristics between clinical and daily life settings in children with cerebral palsy, Sci. Rep. 10 (1) (2020) 1–11.
[8] A. Adeel, M. Gogate, S. Farooq, C. Ieracitano, K. Dashtipour, H. Larijani, A. Hussain, A survey on the role of wireless sensor networks and IoT in disaster management, in: Geological Disaster Monitoring Based on Sensor Networks, Springer, 2019, pp. 57–66.
[9] Y. Y.I.N., Y. Zeng, X. Chen, Y. Fan, The internet of things in healthcare: An overview, J. Ind. Inf. Integr. 1 (2016) 3–13.
[10] J. Jin, J. Gubbi, S. Marusic, M. Palaniswami, An information framework for creating a smart city through internet of things, IEEE Internet Things J. 1 (2) (2014) 112–121.
[11] E. Charry, W. Hu, M. Umer, A. Ronchi, S. Taylor, Study on estimation of peak ground reaction forces using tibial accelerations in running, in: Proceedings of the 2013 IEEE 8th International Conference on Intelligent Sensors, vol. 1, 2013, pp. 288–293.
[12] M. Andries, O. Simonin, F. Charpillet, Localization of humans, objects, and robots interacting on load-sensing floors, IEEE Sensors 16 (2016) 1026–1037.
[13] R. Das, G. Tuna, A. Tuna, Design and implementation of a smart home for the elderly and disabled, Environment 1 (2015) 3.
[14] M. Irfan, H. Jawad, B.B. Felix, S. Farooq Abbasi, A. Nawaz, S. Akbarzadeh, M. Awais, L. Chen, T. Westerlund, W. Chen, Non-wearable IoT-based smart ambient behavior observation system, IEEE Sens. J. 21 (18) (2021) 20857–20869.
[15] B. Pogorelc, M. Gams, Home-based health monitoring of the elderly through gait recognition, J. Ambient Intell. Smart Environ. 4 (5) (2012) 415–428.
[16] Z. Xue, D. Ming, W. Song, B. Wan, S. Jin, Infrared gait recognition based on wavelet transform and support vector machine, Pattern Recognit. 43 (8) (2010) 2904–2910.
[17] M. Goffredo, I. Bouchrika, J.N. Carter, M.S. Nixon, Performance analysis for automated gait extraction and recognition in multi-camera surveillance, Multimedia Tools Appl. 50 (1) (2010) 75–94.
[18] W. Wang, A.X. Liu, M. Shahzad, Gait recognition using wifi signals, in: Proceedings of the 2016 ACM International Joint Conference on Pervasive and Ubiquitous Computing, 2016, pp. 363–373.
[19] L. Middleton, A.A. Buss, A. Bazin, M.S. Nixon, A floor sensor system for gait recognition, in: Fourth IEEE Workshop on Automatic Identification Advanced Technologies AutoID'05, 2005, pp. 171–176.

[20] J.D. Schaafsma, N. Giladi, Y. Balash, A.L. Bartels, T. Gurevich, J.M. Hausdorff, Gait dynamics in Parkinson's disease: relationship to Parkinsonian features, falls and response to levodopa, J. Neurol. Sci. 212 (1–2) (2003) 47–53.
[21] R.G. Ellis, K.C. Howard, R. Kram, The metabolic and mechanical costs of step time asymmetry in walking, Proc. R. Soc. Lond. B Biol. Sci. 280 (1756) (2013) 20122784.
[22] D.P. LaRoche, S.B. Cook, K. Mackala, Strength asymmetry increases gait asymmetry and variability in older women, Med. Sci. Sports Exerc. 44 (11) (2012) 2172.
[23] K.K. Patterson, I. Parafianowicz, C.J. Danells, V. Closson, M.C. Verrier, W.R. Staines, S.E. Black, W.E. McIlroy, Gait asymmetry in community-ambulating stroke survivors, Arch. Phys. Med. Rehabil. 89 (2) (2008) 304–310.
[24] M.D. Lewek, C.E. Bradley, C.J. Wutzke, S.M. Zinder, The relationship between spatiotemporal gait asymmetry and balance in individuals with chronic stroke, J. Appl. Biomech. 30 (1) (2014) 31–36.
[25] M. Alam, A. Garg, T. Munia, R. Fazel-Rezai, K. Tavakolian, Vertical ground reaction force marker for Parkinson's disease, PLoS ONE 12 (2017).
[26] N. A. Code of Federal Regulations, Title 24 room requirements, 2022, https://www.ecfr.gov/current/title-24/subtitle-B/chapter-XX/part-3280/subpart-B/section-3280.109, last accessed 2 May 2022.
[27] J.S. Park, C.M. Lee, S.-M. Koo, C.H. Kim, Gait phase detection using force sensing resistors, IEEE Sens. J. 20 (12) (2020) 6516–6523.
[28] A. Ancillao, S. Tedesco, J. Barton, B. O'Flynn, Indirect measurement of ground reaction forces and moments by means of wearable inertial sensors: A systematic review, Sensors 18 (8) (2018) 2564.
[29] E. Kalkan, An automatic P-phase arrival-time picker, Bull. Seismol. Soc. Am. 106 (3) (2016) 971–986.
[30] K.S. Hahm, A.S. Chase, B. Dwyer, B.W. Anthony, Indoor human localization and gait analysis using machine learning for in-home health monitoring, in: 2021 43rd Annual International Conference of the IEEE Engineering in Medicine & Biology Society, EMBC, 2021, pp. 6859–6862.
[31] D.A. Reynolds, Gaussian mixture models, Encycl. Biom. 741 (659–663) (2009).
[32] G. Leporace, L.A. Batista, L. Metsavaht, J. Nadal, Residual analysis of ground reaction forces simulation during gait using neural networks with different configurations, in: 2015 37th Annual International Conference of the IEEE Engineering in Medicine and Biology Society, EMBC, 2015, pp. 2812–2815.
[33] M. Mirshekari, S. Pan, J. Fagert, E.M. Schooler, P. Zhang, H.Y. Noh, Occupant localization using footstep-induced structural vibration, Mech. Syst. Signal Process. 112 (2018) 77–97.
[34] A.G. Woolard, V.S. Malladi, S. Alajlouni, P.A. Tarazaga, Classification of event location using matched filters via on-floor accelerometers, in: Sensors and Smart Structures Technologies for Civil, Mechanical, and Aerospace Systems 2017, vol. 10168, 2017, p. 101681A.
[35] V. VanderHorst, Private communication, 2021.
[36] J. Cai, J. Luo, S. Wang, S. Yang, Feature selection in machine learning: A new perspective, Neurocomputing 300 (2018) 70–79.
[37] J.D. Schaafsma, N. Giladi, Y. Balash, A.L. Bartels, T. Gurevich, J.M. Hausdorff, Gait dynamics in parkinson's disease: relationship to Parkinsonian features, falls and response to levodopa, J. Neurol. Sci 212 (1–2) (2003) 47–53.
[38] P.A. LeWitt, Levodopa for the treatment of Parkinson's disease, N. Engl. J. Med. 359 (23) (2008) 2468–2476.